ACS chemical biology

Letters

pubs.acs.org/acschemicalbiology

Rheostatic Control of Cas9-Mediated DNA Double Strand Break (DSB) Generation and Genome Editing

John C. Rose,[†] Jason J. Stephany,[‡] Cindy T. Wei,[†] Douglas M. Fowler,*[,‡,∥] and Dustin J. Maly*[,†,§]

[†]Department of Chemistry, University of Washington, Seattle, Washington 98195, United States

[‡]Department of Genome Sciences, University of Washington, Seattle, Washington 98195, United States

[§]Department of Biochemistry, University of Washington, Seattle, Washington 98195, United States

[∥]Department of Bioengineering, University of Washington, Seattle, Washington 98195, United States

Supporting Information

ABSTRACT: We recently reported two novel tools for precisely controlling and quantifying Cas9 activity: a chemically inducible Cas9 variant (ciCas9) that can be rapidly activated by small molecules and a ddPCR assay for time-resolved measurement of DNA double strand breaks (DSB-ddPCR). Here, we further demonstrate the potential of ciCas9 to function as a tunable rheostat for Cas9 function. We show that a new highly potent and selective small molecule activator paired with a more tightly regulated ciCas9 variant expands the range of accessible Cas9 activity levels. We subsequently demonstrate that ciCas9 activity levels can be dose-dependently tuned with a small molecule activator, facilitating rheostatic time-course experiments. These studies provide the first insight into how Cas9-mediated DSB levels correlate with overall editing efficiency. Thus, we demonstrate that ciCas9 and our DSB-ddPCR assay permit the time-resolved study of Cas9 DSB generation and genome editing kinetics at a wide range of Cas9 activity levels.

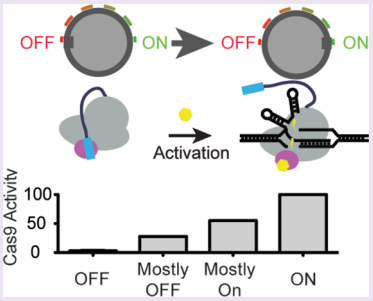

In recent years, CRISPR/Cas9 bacterial immune systems have yielded powerful tools for manipulating and editing the genomes of a wide array of organisms. Insights into the fundamental mechanics of these RNA-guided endonuclease systems—in particular *Streptococcus pyogenes* Cas9—fostered innovations that have improved Cas9 editing efficiency and on-target specificity, as well as broadened the range of targetable sites.[1−6] Further improvements in our understanding of Cas9 biology and biochemistry will likely be useful in tailoring it for a growing number of research, therapeutic, and industrial applications.

We recently reported two new technologies that allowed us to study the kinetics of Cas9-mediated double strand break (DSB) generation and subsequent repair in cells for the first time (Figure 1A,B).[7] First, we developed a novel ddPCR-based assay (DSB-ddPCR) for directly measuring DSBs generated by Cas9. This assay enables quantitative, time-resolved measurement of DSBs at a locus of interest. We also developed an inducible Cas9 variant, chemically inducible Cas9 (ciCas9), that can be rapidly activated with cell-permeable small molecules. Using DSB-ddPCR, we demonstrated that ciCas9 rapidly induces DSBs upon activation and can therefore be used to study DNA cleavage and repair kinetics (Figure 1B). Together, these two tools revealed that cleavage occurs rapidly, with DSBs readily detected as little as 10 min after ciCas9 activation. Indels accrue comparatively slowly, albeit faster than might be expected based on *in vitro* studies.[2,8] Moreover, cleavage and repair kinetics differ between loci, and even between different sgRNAs targeting the same locus.[7]

ciCas9 was developed using a modified intramolecular autoinhibitory strategy that we previously used to engineer chemically inducible activators of GTPases (Figure 1C).[9,10] In this approach, Cas9 activity is autoinhibited by an intramolecular protein−protein interaction between BCL-xL and a BH3 peptide. Upon the addition of a small molecule disruptor of the BCL-xL/BH3 interaction, autoinhibition is released and Cas9 activity is rapidly restored. The single-protein component architecture of ciCas9 suggested that its activity would be conducive to tuning by varying the concentration of the BCL-xL/BH3 disruptor. In effect, ciCas9 could function as a Cas9 rheostat (Figure 1D). We previously demonstrated that the frequency of indels generated by ciCas9 at 24 h is reduced when the concentration of the BCL-xL/BH3 disruptor is lowered. We also showed that strengthening the BCL-xL/BH3 interaction led to reduced basal ciCas9-mediated indel generation but also diminished small molecule-mediated induction of indels. Although these studies only looked at indel generation at a single time point (24 h), they provided the first evidence that ciCas9's activity level could be tuned.

Here, we further explore the potential of ciCas9 to function as a rheostat (Figure 1D,E). We show that A-1155463 (A115, Figure 1), a new and highly potent BCL-xL/BH3 disruptor, yields higher ciCas9 activity than our standard activator of

Special Issue: Chemical Biology of CRISPR

Received: August 1, 2017
Accepted: September 12, 2017
Published: September 12, 2017

DOI: 10.1021/acschembio.7b00652
ACS Chem. Biol. 2018, 13, 438−442

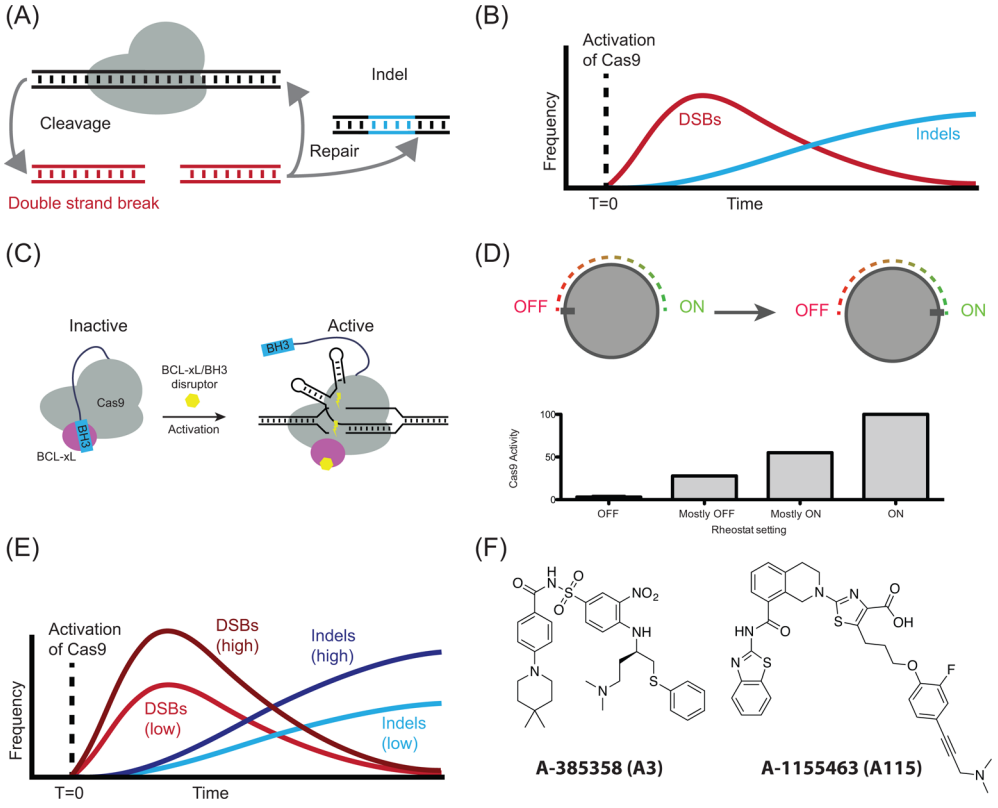

Figure 1. Using a Cas9 rheostat to investigate genome editing kinetics. (A) Cas9 (gray) generates a double strand break (DSB) in DNA, which is subsequently repaired yielding an indel or regenerating the original target sequence. (B) Temporally precise induction of chemically inducible Cas9 (ciCas9) activity enables kinetic study of genome editing by defining $T = 0$. DSB-ddPCR and high-throughput DNA sequencing can be used to monitor the frequency of DSBs and indels over time after induction of ciCas9 activity at $T = 0$. (C) ciCas9 is a single-component engineered Cas9 variant that is autoinhibited by the BCL-xL/BH3 interaction in the basal state. Upon the addition of small molecule disruptors of the BCL-xL/BH3 interaction, ciCas9 is activated. (D) Dose-dependent activation of ciCas9 by small molecule BCL-xL/BH3 disruptors allows tunable activation of genome editing activity, thereby acting as a Cas9 rheostat. (E) The temporal precision and tunability of ciCas9 activation—coupled with DSB-ddPCR and high-throughput DNA sequencing—permit examination of the relationship between Cas9 activity level, DSB generation, and the appearance of indels over time. (F) Chemical structures of the BCL-xL/BH3 disruptors A3 and A115.

ciCas9.[11] Furthermore, A115 enables robust activation of a more tightly autoinhibited ciCas9 variant. Together, the more potent A115 and the more tightly autoinhibited ciCas9 variant offer an expanded range of readily accessible Cas9 activity levels. We also show that by altering the concentration of a disruptor of intermediate potency, we can tune ciCas9 activity levels. We take advantage of this rheostatic control to precisely tune Cas9 activity and find that ciCas9-mediated DSB levels at an early time point correlate well with overall editing efficiency after 24 h. Our rheostatic study provides a first glimpse into the temporal relationship between Cas9 activity level, DSB generation, and indel appearance and serves as a framework for systematically determining the inter-relationship between these parameters at different sites in the genome.

We previously demonstrated that using BCL-xL/BH3 disruptors more potent than our standard ciCas9 activator A-385358 ("A3") led to a relative overall increase in indels 24 h after ciCas9 activation.[7] On the basis of these results, we were particularly interested in exploring the level of activity conferred by A115. A115 is the most potent BCL-xL/BH3 disruptor reported to date, with a low picomolar affinity for BCL-xL.[11] A115 is also highly selective for BCL-xL (>1000-fold lower affinity for BCL-2, BCL-W, and MCL-1). Furthermore, we recently found that A-115 is more effective than A3 in activating an inducible RAS activator that relies on a similar BCL-xL/BH3 autoinhibition strategy (unpublished data). Thus, we expected that A115 would yield enhanced ciCas9 activity, compared to A3.

To investigate the effects of A115 on ciCas9-mediated DSB generation and subsequent indel appearance, HEK-293T cells were transfected with plasmids encoding AAVS1 sgRNA and ciCas9. The AAVS1 locus was selected because it is a well-characterized "safe-harbor" locus, in which editing is unlikely to have deleterious effects.[12,13] Cells were then treated with 10 μM A3 or the more potent A115. Samples were taken 1, 2, and 24 h after BCL-xL/BH3 disruptor treatment. DSB frequencies were determined using DSB-ddPCR, and indel frequencies were measured using high throughput sequencing (Figure 2). We note that we fit our DSB-ddPCR data to a standard curve that we generated by mixing different amounts of control cleaved and uncleaved template DNA. While fitting DSB-ddPCR data to a standard curve increases accuracy, it can lead to the small negative values we observed (Figure 2). In cells transfected with ciCas9, both A3 and A115 led to robust increases in ciCas9-induced DSBs (Figure 2A), with A115 inducing a faster accumulation of DSBs over the first 2 h. Between 2 and 24 h, DSB frequency declined in cells treated with A3. In contrast, the high frequency of DSBs induced by A115 at 2 h persisted until at least 24 h. The higher frequency of DSBs generated by A115 at earlier time points translated into a higher degree of indel generation at 24 h relative to A3 (Figure 2B). Thus, 10 μM A3 appears to only partially disrupt

DOI: 10.1021/acschembio.7b00652
ACS Chem. Biol. 2018, 13, 438−442

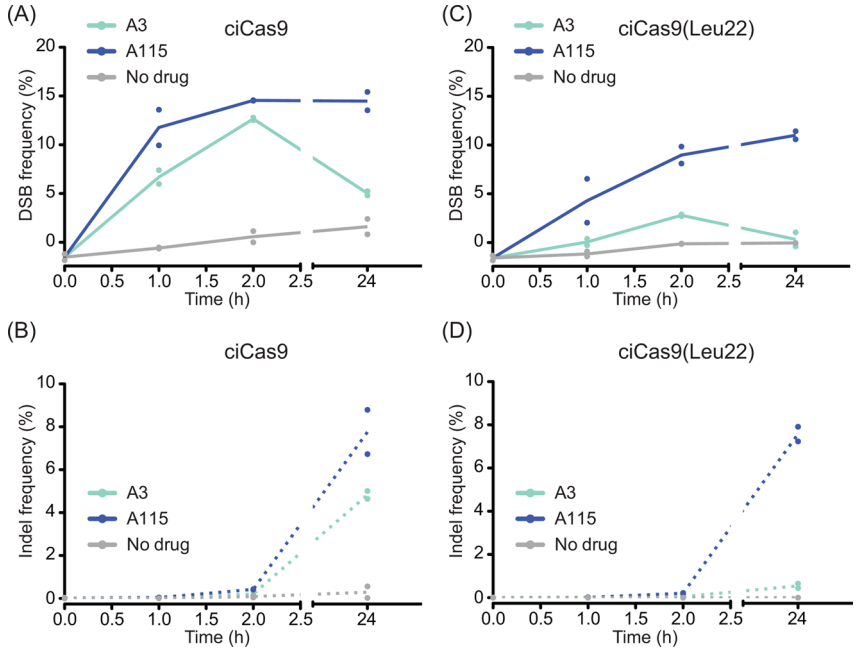

Figure 2. Activation of ciCas9 and ciCas9(Leu22) using a potent BCL-xL/BH3 disruptor, A-115463. (A,B) Time course of (A) DSB frequencies as determined by DSB-ddPCR and (B) indel frequencies as determined by high-throughput DNA sequencing following activation of ciCas9. HEK-293T cells transfected with plasmids encoding ciCas9 and AAVS1 sgRNA were treated with A3 (10 μM) or A115 (10 μM). (C,D) Time course of (C) DSB frequencies as determined by DSB-ddPCR and (D) indel frequencies as determined by high-throughput sequencing after activation of the more tightly autoinhibited ciCas9 variant, ciCas9(Leu22). HEK-293T cells transfected with plasmids encoding ciCas9(Leu22) and AAVS1 sgRNA were treated with A3 (10 μM) or A115 (10 μM). Individual cell culture replicates are shown. Lines connect means of two (n = 2) cell culture replicates, except n = 1 for ciCas9(Leu22), no drug addition, at 24 h.

the BCL-xL/BH3 interaction, leading to incomplete activation of ciCas9. The same concentration of the more potent A115 disrupts the interaction further. The resulting A115-driven decrease in intramolecular autoinhibition leads to faster generation of DSBs and, subsequently, an increased level of indels at 24 h.

In our previous work, we determined that the basal activity of ciCas9 can be readily tailored by altering its sequence. For example, we found that mutating a single BH3 residue yielded variants with a higher intramolecular affinity for BCL-xL. ciCas9 variants containing these higher-affinity BH3 sequences exhibited decreased basal activity in the absence of a BCL-xL/BH3 disruptor. Unfortunately, this reduced basal activity was accompanied by a decrease in disruptor-induced activation. Therefore, we examined whether the more potent A115 could lead to more robust activation of one of these highly autoinhibited constructs, ciCas9(Leu22).

HEK-293T cells were transfected with plasmids encoding AAVS1 sgRNA and ciCas9(Leu22), and DSB and indel frequencies were measured after treatment with either 10 μM A3 or A115. Consistent with our previous observations, ciCas9(Leu22) led to no appreciable accrual of indels in the absence of a disruptor (Supporting Information Figure 1).[7] Activation of ciCas9(Leu22) with A3 produced a modest increase in DSBs that peaked after 2 h (Figure 2B), and few indels were observed after 24 h (Figure 2D). Treatment of ciCas9(Leu22) with A115, on the other hand, led to rapid induction of DSBs, albeit at approximately half the initial rate observed relative to wild type ciCas9 activated with A115. Furthermore, unlike wild type ciCas9, ciCas9(Leu22)-mediated DSB generation continued to increase even at 24 h. Despite the differences in DSB kinetics when ciCas9 and ciCas9(Leu22) were activated with A115, both yielded similar levels of indels at 24 h (Figure 2D). Thus, the slower rate of initial activation of ciCas9(Leu22) by A115 did not appear to affect indel frequency at the later 24 h time point.

The persistence of unresolved DSBs in A115-treated cells as compared to A3-treated cells at 24 h for both ciCas9 and ciCas9(Leu22) is particularly surprising. Time courses were performed without a "wash-out" step, and both disruptors would be expected to be stable over 24 h of cell culture (*e.g.*, we previously demonstrated that A3 can drive an inducible RAS activator for at least 48 h).[10] Thus, the observed difference is unlikely to be due to a difference in disruptor concentration during the course of the experiment. Potentially, tighter binding of A115 to BCL-xL may yield a more stable ciCas9·sgRNA·DSB complex. The greater stability of this complex relative to that induced by A3 may lead to increased DSB persistence as the ternary complex with ciCas9 and sgRNA shields the DSB from DNA repair factors such as Ku. However, further experiments will be needed to understand this effect. Together, these studies demonstrate that an expanded dynamic range of accessible editing activities can be achieved by tuning ciCas9 autoinhibition and BCL-xL/BH3 disruptor potency. In particular, combining a more tightly autoinhibited ciCas9 variant with a more potent BCL-xL/BH3 disruptor enabled robust induced activity in the context of low basal activity. Furthermore, the use of BCL-xL/BH3 disruptors with differing binding affinities and kinetics may allow us to infer mechanistic details and biochemical properties of the Cas9-mediated cleavage and repair process that have so far proved elusive.

Understanding the dynamic relationship between Cas9 activity level, DSB generation, and indel appearance requires inducible, tunable control of Cas9 activity. Thus, we conducted ciCas9 time course experiments at a range of BCL-xL/BH3 disruptor concentrations, measuring DSB and indel frequencies

DOI: 10.1021/acschembio.7b00652
ACS Chem. Biol. 2018, 13, 438−442

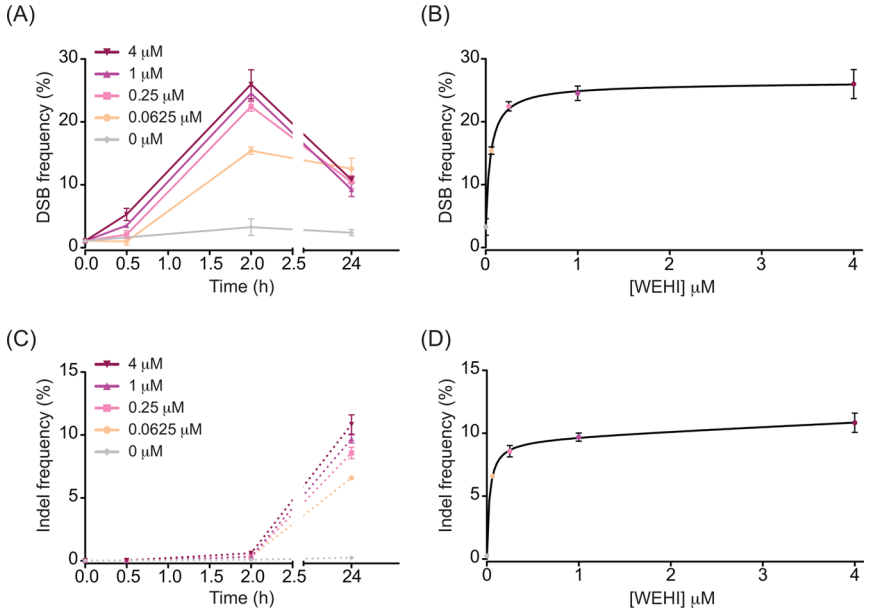

Figure 3. DSB and indel frequencies vary over time in response to differing degrees of ciCas9 activity. (A) Time course of DSB frequencies as determined by DSB-ddPCR following activation of ciCas9 with a range of concentrations of the WEHI-539 disruptor. HEK-293T cells transfected with plasmids encoding ciCas9 and AAVS1 sgRNA were treated with a range of concentrations of WEHI-539 (0–4 μM). (B) WEHI-539 dose dependence of DSB frequency at 2 h. (C) Indel frequencies for time course in A as determined by high-throughput DNA sequencing following activation of ciCas9 with a range of concentrations of WEHI-539. (D) WEHI dose dependence of indel frequency at 24 h. Error bars = SEM (n = 3 cell culture replicates).

over time. We selected WEHI-539,[14] which we previously showed could activate ciCas9, as the disruptor for a dose–response study because it displays intermediate cellular potency relative to A3 and A115. This intermediate potency makes it an ideal candidate for exploring a range of ciCas9 activity levels. HEK-293T cells were transfected with plasmids encoding ciCas9 and AAVS1 sgRNA. Cells were treated with varying concentrations of WEHI-539 and DSB, and indel frequencies were determined at 0.5, 2, and 24 h after drug treatment (Figure 3, Supporting Information Figure 2). Consistent with our previous work, in the absence of any drug, ciCas9 did not yield an appreciable increase in DSBs at this locus throughout the time course (Figure 3A). The addition of increasing concentrations of WEHI-539 led to an increase in DSBs over the first 2 h of the time course. The difference in DSB frequency between drug concentrations was most pronounced at 30 min. DSB frequencies for all drug concentrations reach a maximum at 2 h.

After 2 h, DSB frequencies for cells treated with 0.25–4 μM WEHI decreased significantly. However, we observed, at most, a modest decline in DSB frequency for cells treated with the lowest concentration of WEHI (0.063 μM) over this time period. Consequently, while the three higher concentrations elicited higher maximum DSB frequencies at 2 h (22.5–26.0%, compared to 15.4% for 0.0625 μM, Figure 3B), the frequency of DSBs was similar for all four concentrations of WEHI-539 at 24 h (9.3–12.5%). Despite the apparently complex relationship between ciCas9 activity and DSB kinetics, the indel frequency at 24 h demonstrated a clear dose-dependent increase (Figure 3C). Interestingly, the relationship between WEHI-539 concentration and DSB frequency at 2 h appears remarkably similar to the relationship between WEHI-539 concentration and indel frequency at 24 h (Figure 3B,D). Thus, the ability of ciCas9 to generate DSBs at an early time point is predictive of subsequent indels at 24 h.

In summary, we describe the use of ciCas9 and DSB-ddPCR to control and examine the effects of varied levels of genome editing activity over time. We demonstrate that a highly potent BCL-xL/BH3 disruptor, A-1155463, and a more tightly autoinhibited ciCas9 variant, ciCas9(Leu22), expand the dynamic range of editing activity that can be accessed. Going forward, the use of A-115 with ciCas9(Leu22) provides an optimal system for obtaining robust editing with minimal basal activity.

We also show that we can achieve fine-grained control of ciCas9-mediated genome editing activity by varying the concentration of a BCL-xL/BH3 disruptor of intermediate potency. We leverage this control of ciCas9 activity by making time-resolved, quantitative measurements of DSB and indel frequencies to collect "rheostatic timecourses." In a systematic study of the AAVS1 locus, we find that there is a remarkable correlation between ciCas9-mediated DSB levels at an early time point and overall editing after 24 h. In the future, the precise rheostatic control we have achieved over the degree and timing of Cas9-mediated editing activity will permit precise dissection of the cleavage and repair process at numerous loci. In particular, ciCas9 could be used to test, refine, and expand hypotheses regarding the Cas9 mechanism and kinetics generated by *in vitro*[2,8,15,16] and computational studies.[17] For instance, May and colleagues recently characterized the genome-wide landscape of off-target cutting by Cas9 *in vitro*.[16] Increasing the concentration of the Cas9·gRNA complex resulted in an increasing number of off-target cleavage events. The rheostatic control afforded by ciCas9 enables analogous experiments in cells or *in vivo*, which would help to quantitatively decipher the dependence of off-target editing on the magnitude of Cas9 activity. May and colleagues also examined the role of the duration of Cas9 exposure in cells on off-target editing, but the temporal resolution was limited to a scale of several days to weeks.[16] ciCas9 and DSB-ddPCR would

DOI: 10.1021/acschembio.7b00652
ACS Chem. Biol. 2018, 13, 438–442

allow examination of the kinetics of off-target DSBs and indels with a resolution on the order of minutes. The insights gleaned from this and other future work may lead to novel approaches for enhancing editing efficiency or specificity.

Beyond studies of the editing process itself, rheostatic control of Cas9 activity would permit greater control of a wide range of genome editing applications. For instance, ciCas9 could be used to control the timing and the rate of knockout of a tumor suppressor *in vivo* for examinations of tumorigenesis. Precise adjustment of ciCas9 activity levels could be used to control editing zygosity, enabling preferential generation of homo- or heterozygotes. Facile, temporal control of gene knockout could also be of great utility in studies of development. Thus, our findings expand our ability to manipulate and investigate Cas9-mediated genome editing in cells.

METHODS

Details of experimental procedures are provided in the Supporting Information.

ASSOCIATED CONTENT

Supporting Information

The Supporting Information is available free of charge on the ACS Publications website at DOI: 10.1021/acschembio.7b00652.

Methods section and supporting figures (PDF)

AUTHOR INFORMATION

Corresponding Authors

*Tel.: 206-221-5711. E-mail: dfowler@uw.edu.
*Tel.: 206-543-1653. E-mail: djmaly@uw.edu.

ORCID

Dustin J. Maly: 0000-0003-0094-0177

Funding

This work was supported by the National Institutes of Health (R01GM086858 (D.J.M), R01GM109110 (D.M.F), F30CA189793 (J.C.R)) and NSF (0954242 (D.J.M)).

Notes

The authors declare no competing financial interest.

ACKNOWLEDGMENTS

We would like to thank W. Valente and J. Bielas for technical assistance.

REFERENCES

(1) Fu, Y., Sander, J. D., Reyon, D., Cascio, V. M., and Joung, J. K. (2014) Improving CRISPR-Cas nuclease specificity using truncated guide RNAs. *Nat. Biotechnol. 32*, 279−284.

(2) Richardson, C. D., Ray, G. J., DeWitt, M. A., Curie, G. L., and Corn, J. E. (2016) Enhancing homology-directed genome editing by catalytically active and inactive CRISPR-Cas9 using asymmetric donor DNA. *Nat. Biotechnol. 34*, 339−344.

(3) Slaymaker, I. M., Gao, L., Zetsche, B., Scott, D. A., Yan, W. X., and Zhang, F. (2016) Rationally engineered Cas9 nucleases with improved specificity. *Science 351*, 84−88.

(4) Kleinstiver, B. P., Pattanayak, V., Prew, M. S., Tsai, S. Q., Nguyen, N. T., Zheng, Z., and Joung, J. K. (2016) High-fidelity CRISPR-Cas9 nucleases with no detectable genome-wide off-target effects. *Nature 529*, 490−495.

(5) Suzuki, K., Tsunekawa, Y., Hernandez-Benitez, R., Wu, J., Zhu, J., Kim, E. J., Hatanaka, F., Yamamoto, M., Araoka, T., Li, Z., Kurita, M., Hishida, T., Li, M., Aizawa, E., Guo, S., Chen, S., Goebl, A., Soligalla, R. D., Qu, J., Jiang, T., Fu, X., Jafari, M., Esteban, C. R., Berggren, W. T., Lajara, J., Nunez-Delicado, E., Guillen, P., Campistol, J. M., Matsuzaki, F., Liu, G. H., Magistretti, P., Zhang, K., Callaway, E. M., Zhang, K., and Belmonte, J. C. (2016) In vivo genome editing via CRISPR/Cas9 mediated homology-independent targeted integration. *Nature 540*, 144−149.

(6) Kleinstiver, B. P., Prew, M. S., Tsai, S. Q., Nguyen, N. T., Topkar, V. V., Zheng, Z., and Joung, J. K. (2015) Broadening the targeting range of Staphylococcus aureus CRISPR-Cas9 by modifying PAM recognition. *Nat. Biotechnol. 33*, 1293−1298.

(7) Rose, J. C., Stephany, J. J., Valente, W. J., Trevillian, B. M., Dang, H. V., Bielas, J. H., Maly, D. J., and Fowler, D. M. (2017) Rapidly inducible Cas9 and DSB-ddPCR to probe editing kinetics. *Nat. Methods 14*, 891−896.

(8) Sternberg, S. H., Redding, S., Jinek, M., Greene, E. C., and Doudna, J. A. (2014) DNA interrogation by the CRISPR RNA-guided endonuclease Cas9. *Nature 507*, 62−67.

(9) Goreshnik, I., and Maly, D. J. (2010) A small molecule-regulated guanine nucleotide exchange factor. *J. Am. Chem. Soc. 132*, 938−940.

(10) Rose, J. C., Huang, P. S., Camp, N. D., Ye, J., Leidal, A. M., Goreshnik, I., Trevillian, B. M., Dickinson, M. S., Cunningham-Bryant, D., Debnath, J., Baker, D., Wolf-Yadlin, A., and Maly, D. J. (2016) A computationally engineered RAS rheostat reveals RAS-ERK signaling dynamics. *Nat. Chem. Biol. 13*, 119−126.

(11) Tao, Z. F., Hasvold, L., Wang, L., Wang, X., Petros, A. M., Park, C. H., Boghaert, E. R., Catron, N. D., Chen, J., Colman, P. M., Czabotar, P. E., Deshayes, K., Fairbrother, W. J., Flygare, J. A., Hymowitz, S. G., Jin, S., Judge, R. A., Koehler, M. F., Kovar, P. J., Lessene, G., Mitten, M. J., Ndubaku, C. O., Nimmer, P., Purkey, H. E., Oleksijew, A., Phillips, D. C., Sleebs, B. E., Smith, B. J., Smith, M. L., Tahir, S. K., Watson, K. G., Xiao, Y., Xue, J., Zhang, H., Zobel, K., Rosenberg, S. H., Tse, C., Leverson, J. D., Elmore, S. W., and Souers, A. J. (2014) Discovery of a Potent and Selective BCL-XL Inhibitor with in Vivo Activity. *ACS Med. Chem. Lett. 5*, 1088−1093.

(12) Sadelain, M., Papapetrou, E. P., and Bushman, F. D. (2011) Safe harbours for the integration of new DNA in the human genome. *Nat. Rev. Cancer 12*, 51−58.

(13) DeKelver, R. C., Choi, V. M., Moehle, E. A., Paschon, D. E., Hockemeyer, D., Meijsing, S. H., Sancak, Y., Cui, X., Steine, E. J., Miller, J. C., Tam, P., Bartsevich, V. V., Meng, X., Rupniewski, I., Gopalan, S. M., Sun, H. C., Pitz, K. J., Rock, J. M., Zhang, L., Davis, G. D., Rebar, E. J., Cheeseman, I. M., Yamamoto, K. R., Sabatini, D. M., Jaenisch, R., Gregory, P. D., and Urnov, F. D. (2010) Functional genomics, proteomics, and regulatory DNA analysis in isogenic settings using zinc finger nuclease-driven transgenesis into a safe harbor locus in the human genome. *Genome Res. 20*, 1133−1142.

(14) Lessene, G., Czabotar, P. E., Sleebs, B. E., Zobel, K., Lowes, K. N., Adams, J. M., Baell, J. B., Colman, P. M., Deshayes, K., Fairbrother, W. J., Flygare, J. A., Gibbons, P., Kersten, W. J., Kulasegaram, S., Moss, R. M., Parisot, J. P., Smith, B. J., Street, I. P., Yang, H., Huang, D. C., and Watson, K. G. (2013) Structure-guided design of a selective BCL-X(L) inhibitor. *Nat. Chem. Biol. 9*, 390−397.

(15) Boyle, E. A., Andreasson, J. O. L., Chircus, L. M., Sternberg, S. H., Wu, M. J., Guegler, C. K., Doudna, J. A., and Greenleaf, W. J. (2017) High-throughput biochemical profiling reveals sequence determinants of dCas9 off-target binding and unbinding. *Proc. Natl. Acad. Sci. U. S. A. 114*, 5461−5466.

(16) Cameron, P., Fuller, C. K., Donohoue, P. D., Jones, B. N., Thompson, M. S., Carter, M. M., Gradia, S., Vidal, B., Garner, E., Slorach, E. M., Lau, E., Banh, L. M., Lied, A. M., Edwards, L. S., Settle, A. H., Capurso, D., Llaca, V., Deschamps, S., Cigan, M., Young, J. K., and May, A. P. (2017) Mapping the genomic landscape of CRISPR-Cas9 cleavage. *Nat. Methods 14*, 600−606.

(17) Farasat, I., and Salis, H. M. (2016) A Biophysical Model of CRISPR/Cas9 Activity for Rational Design of Genome Editing and Gene Regulation. *PLoS Comput. Biol. 12*, e1004724.

DOI: 10.1021/acschembio.7b00652
ACS Chem. Biol. 2018, 13, 438−442